

# Did the COVID-19 Crisis Reduce Free Tropospheric Ozone across the Northern Hemisphere?

Wolfgang Steinbrecht<sup>1</sup>, Dagmar Kubistin<sup>1</sup>, Christian Plass-Dülmer<sup>1</sup>, Jonathan Davies<sup>2</sup>, David W. Tarasick<sup>2</sup>, Peter von der Gathen<sup>3</sup>, Holger Deckelmann<sup>3</sup>, Nis Jepsen<sup>4</sup>, Rigel Kivi<sup>5</sup>, Norrie Lyall<sup>6</sup>, Matthias Palm<sup>7</sup>, Justus Notholt<sup>7</sup>, Bogumil Kois<sup>8</sup>, Peter Oelsner<sup>9</sup>, Marc Allaart<sup>10</sup>, Ankie Piters<sup>10</sup>, Michael Gill<sup>11</sup>, Roeland Van Malderen<sup>12</sup>, Andy W. Delcloo<sup>12</sup>, Ralf Sussmann<sup>13</sup>, Emmanuel Mahieu<sup>14</sup>, Christian Servais<sup>14</sup>, Gonzague Romanens<sup>15</sup>, Rene Stübi<sup>15</sup>, Gerard Ancellet<sup>16</sup>, Sophie Godin-Beekmann<sup>16</sup>, Shoma Yamanouchi<sup>17</sup>, Kimberly Strong<sup>17</sup>, Bryan Johnson<sup>18</sup>, Patrick Cullis<sup>18,19</sup>, Irina Petropavlovskikh<sup>18,19</sup>, James W. Hannigan<sup>20</sup>, Jose-Luis Hernandez<sup>21</sup>, Ana Diaz Rodriguez<sup>21</sup>, Tatsumi Nakano<sup>22</sup>, Fernando Chouza<sup>23</sup>, Thierry Leblanc<sup>23</sup>, Carlos Torres<sup>24</sup>, Omaira Garcia<sup>24</sup>, Amelie N. Röhlings<sup>25</sup>, Matthias Schneider<sup>25</sup>, Thomas Blumenstock<sup>25</sup>, Matt Tully<sup>26</sup>, Clare Paton-Walsh<sup>27</sup>, Nicholas Jones<sup>27</sup>, Richard Querel<sup>28</sup>, Susan Strahan<sup>29,30</sup>, Ryan M. Stauffer<sup>29,33</sup>, Anne M. Thompson<sup>29</sup>, Antje Inness<sup>31</sup>, Richard Engelen<sup>31</sup>, Kai-Lan Chang<sup>32,19</sup>, Owen R. Cooper<sup>32,19</sup>

<sup>1</sup>Deutscher Wetterdienst, Hohenpeißenberg, Germany.

<sup>2</sup>Environment and Climate Change Canada, Toronto, Canada.

<sup>3</sup>Alfred Wegener Institut, Helmholtz-Zentrum für Polar- und Meeresforschung, Potsdam, Germany.

<sup>4</sup>Danish Meteorological Institute, Copenhagen, Denmark.

<sup>5</sup>Finnish Meteorological Institute, Sodankylä, Finland.

<sup>6</sup>British Meteorological Service, Lerwick, United Kingdom.

<sup>7</sup>University of Bremen, Bremen, Germany.

<sup>8</sup>Institute of Meteorology and Water Management, Legionowo, Poland.

<sup>9</sup>Deutscher Wetterdienst, Lindenberg, Germany.

<sup>10</sup>Royal Netherlands Meteorological Institute, DeBilt, The Netherlands.

<sup>11</sup>Met Éireann (Irish Met. Service), Valentia, Ireland.

<sup>12</sup>Royal Meteorological Institute of Belgium, Uccle, Belgium.

<sup>13</sup>Karlsruhe Institute of Technology, IMK-IFU, Garmisch-Partenkirchen, Germany.

<sup>14</sup>Institute of Astrophysics and Geophysics, University of Liège, Liège, Belgium.

<sup>15</sup>Federal Office of Meteorology and Climatology, MeteoSwiss, Payerne, Switzerland.

<sup>16</sup>LATMOS, Sorbonne Université-UVSQ-CNRS/INSU, Paris, France.

<sup>17</sup>University of Toronto, Toronto, Canada.

<sup>18</sup>NOAA ESRL Global Monitoring Laboratory, Boulder, CO, USA.

<sup>19</sup>Cooperative Institute for Research in Environmental Sciences (CIRES), University of Colorado, Boulder, CO, USA.

37 <sup>20</sup>National Center for Atmospheric Research, Boulder, CO, USA.

38 <sup>21</sup>State Meteorological Agency (AEMET), Madrid, Spain.

39 <sup>22</sup>Meteorological Research Institute, Tsukuba, Japan.

40 <sup>23</sup>Jet Propulsion Laboratory, California Institute of Technology, Table Mountain Facility,  
41 Wrightwood, CA, USA.

42 <sup>24</sup>Izaña Atmospheric Research Center, AEMET, Tenerife, Spain.

43 <sup>25</sup>Karlsruhe Institute of Technology, IMK-ASF, Karlsruhe, Germany.

44 <sup>26</sup>Bureau of Meteorology, Melbourne, Australia.

45 <sup>27</sup>Centre for Atmospheric Chemistry, University of Wollongong, Wollongong, Australia.

46 <sup>28</sup>National Institute of Water and Atmospheric Research, Lauder, New Zealand.

47 <sup>29</sup>Earth Sciences Division, NASA Goddard Space Flight Center, Greenbelt, MD, USA.

48 <sup>30</sup>Universities Space Research Association, Columbia, MD, USA.

49 <sup>31</sup>European Centre for Medium-Range Weather Forecasts, Reading, United Kingdom.

50 <sup>32</sup>NOAA Chemical Sciences Laboratory, Boulder, CO, USA.

51 <sup>33</sup>Earth System Science Interdisciplinary Center, University of Maryland, College Park, MD,  
52 USA

53

54 Corresponding author: Wolfgang Steinbrecht ([wolfgang.steinbrecht@dwd.de](mailto:wolfgang.steinbrecht@dwd.de))

55

56 **Key Points (shortened to less than 140 characters each, and changed as suggested by**  
57 **Reviewer #2):**

- 58     • In spring and summer 2020, stations in the northern extratropics report on average 7% (4  
59     nmol/mol) less tropospheric ozone than normal.
- 60     • Such low tropospheric ozone, over several months, and at so many sites, has not been  
61     observed in any previous year since at least 2000.
- 62     • Most of the reduction in tropospheric ozone in 2020 is likely due to emissions reductions  
63     related to the COVID-19 pandemic.
- 64

## 65 **Abstract**

66 Throughout spring and summer 2020, ozone stations in the northern extratropics recorded  
67 unusually low ozone in the free troposphere. From April to August, and from 1 to 8 kilometers  
68 altitude, ozone was on average 7% ( $\approx 4$  nmol/mol) below the 2000 to 2020 climatological mean.  
69 Such low ozone, over several months, and at so many stations, has not been observed in any  
70 previous year since at least 2000. Atmospheric composition analyses from the Copernicus  
71 Atmosphere Monitoring Service and simulations from the NASA GMI model indicate that the  
72 large 2020 springtime ozone depletion in the Arctic stratosphere contributed less than one  
73 quarter of the observed tropospheric anomaly. The observed anomaly is consistent with recent  
74 chemistry-climate model simulations, which assume emissions reductions similar to those caused  
75 by the COVID-19 crisis. COVID-19 related emissions reductions appear to be the major cause  
76 for the observed reduced free tropospheric ozone in 2020.

77

## 78 **Plain Language Summary**

79 Worldwide actions to contain the COVID-19 virus have closed factories, grounded airplanes, and  
80 have generally reduced travel and transportation. Less fuel was burnt, and less exhaust was  
81 emitted into the atmosphere. Due to these measures, the concentration of nitrogen oxides and  
82 volatile organic compounds (VOCs) decreased in the atmosphere. These substances are  
83 important for photochemical production and destruction of ozone in the atmosphere. In clean or  
84 mildly polluted air, reducing nitrogen oxides and/or VOCs will reduce the photochemical  
85 production of ozone and result in less ozone. In heavily polluted air, in contrast, reducing  
86 nitrogen oxides can increase ozone concentrations, because less nitrogen oxide is available to  
87 destroy ozone. In this study, we use data from three types of ozone instruments, but mostly from  
88 ozonesondes on weather balloons. The sondes fly from the ground up to 30 kilometers altitude.  
89 In the first 8 kilometers, we find significantly reduced ozone concentrations in the northern  
90 extratropics during spring and summer of 2020, less than in any other year since at least 2000.  
91 We suggest that reduced emissions due to the COVID-19 crisis have lowered photochemical  
92 ozone production and have caused the observed ozone reductions in the troposphere.

93

## 94 **1 Introduction**

95 Widespread measures to contain the COVID-19 pandemic have slowed, or even closed  
96 down, industries, businesses, and transportation activities, and have reduced anthropogenic  
97 emissions substantially throughout the year 2020. Guevara et al. (2020), or Barré et al. (2020)  
98 report European emissions reductions up to 60% for  $\text{NO}_x$ , and up to 15% for Non-Methane  
99 Volatile Organic Compounds (NMVOC) in March/April 2020. Based on satellite observations of  
100  $\text{NO}_2$  columns (Bouwens et al., 2020), comparable  $\text{NO}_x$  emissions reductions are reported for  
101 Chinese cities in February 2020 (Ding et al., 2020; Feng et al., 2020). Globally averaged  $\text{CO}_2$   
102 emissions decreased by 8.8% during the first half of 2020 (Liu et al., 2020), consistent in timing  
103 and magnitude with the aforementioned  $\text{NO}_2$  emission reductions. The largest relative reductions  
104 occurred for air traffic, where emissions decreased by  $\approx 40\%$ , on average, in the first half of 2020  
105 (Le Quéré et al., 2020a; Liu et al., 2020), and remained low during the second half of 2020 (Le  
106 Quéré et al., 2020b).

107 These COVID-19 emissions reductions are large enough to affect ozone levels in the  
108 troposphere (Dentener et al., 2011). Tropospheric O<sub>3</sub>-NO<sub>x</sub>-VOC-HO<sub>x</sub> chemistry is, however,  
109 complex and nonlinear. The net effect of emission changes depends on NO<sub>x</sub> and VOC  
110 concentrations (e.g., Kroll et al., 2020; Sillman, 1999; Thornton et al., 2002). In polluted regions,  
111 at high NO<sub>x</sub> concentrations (>> 1ppb), reducing NO<sub>x</sub> concentrations can increase ozone, because  
112 ozone titration by NO is reduced (e.g., Sicard et al., 2020). At low concentrations (NO<sub>x</sub> < 1  
113 nmol/mol), however, in the clean or mildly polluted free troposphere, reducing NO<sub>x</sub> lowers  
114 photochemical ozone production (e.g., Bozem et al., 2017), and results in less ozone.

115 Indeed, for many polluted regions, studies report increased near-surface ozone after  
116 COVID-19 lockdowns (e.g., Collivignarelli et al., 2020; Lee et al., 2020; Shi & Brasseur, 2020;  
117 Siciliano et al., 2020; Venter et al., 2020). Reduced surface ozone is reported for some rural  
118 areas, e.g., in the US and Western Europe (Chen et al., 2020; Menut et al., 2020). Meteorological  
119 conditions complicate matters, as they play an important role as well (Goldberg et al., 2020;  
120 Keller et al., 2020; Ordóñez et al., 2020; Shi & Brasseur, 2020).

121 In the free troposphere, ozone is an important greenhouse gas, and plays a key role in  
122 tropospheric chemical reactions, controlling the oxidizing capacity (e.g. Archibald et al., 2020;  
123 Cooper et al., 2014; Gaudel et al., 2018). The Northern Hemisphere free troposphere is dominated  
124 by net photochemical ozone production, proportional (albeit nonlinearly) to the availability of  
125 ozone precursor gases (e.g., Zhang et al., 2020). In contrast to increases of surface ozone in  
126 polluted urban areas after the COVID-19 emissions reductions, we find significant reductions of  
127 ozone in the northern extratropical free troposphere. These large-scale reductions occurred in late  
128 spring and summer 2020, following the widespread COVID-19 slowdowns, and are unique  
129 within the last two decades.

## 130 **2 Instruments and Data**

131 Regular observations of ozone in the free troposphere are sparse: Only around 50 ozone  
132 sounding stations worldwide (e.g. Tarasick et al., 2019), a handful of tropospheric lidars (Gaudel  
133 et al., 2015; Leblanc et al., 2018), and about twenty Fourier Transform Infrared Spectrometers  
134 (FTIRs, Vigouroux et al., 2015). In-Service Aircraft for a Global Observing System (IAGOS,  
135 Nédélec et al., 2015) are another important source of tropospheric ozone data. Due to the  
136 COVID-19 slowdowns, however, few IAGOS aircraft were flying in 2020, and IAGOS data  
137 became quite sparse, with only about 20 flights per month since April 2020, compared to more  
138 than 200 flights per month in 2019. The information content of satellite measurements on ozone  
139 in the free troposphere is limited, and accuracy is modest, 10 to 30% (Hurtmans et al., 2012; Liu  
140 et al., 2010; Oetjen et al., 2014). The recent Tropospheric Ozone Assessment Report found large  
141 differences in tropospheric ozone trends derived from different satellite instruments, and even  
142 different signs in some regions (Gaudel et al., 2018).

143 Ozonesondes measure profiles with high vertical resolution, about 100 m, and good  
144 accuracy, 5 to 15% in the troposphere, 5% in the stratosphere (Smit et al., 2007; Sterling et al.,  
145 2018; Tarasick et al., 2016; Van Malderen et al., 2016; Witte et al., 2017; WMO, 2014). This is  
146 adequate to detect ozone anomalies of several percent. We use stations with regular soundings, at  
147 least once per month since the year 2000, and with data available until at least July 2020.  
148 Soundings with obvious deficiencies were rejected (i.e. large data gaps, integrated ozone column  
149 from the sounding deviating by more than 30% from ground- or satellite-based spectrometer  
150 measurement). Table 1 provides information on stations, and public data archives.

151  
152

153 **Table 1.** Stations in this study, mostly ozonesonde stations. *FTIR and LIDAR stations are*  
 154 *italicized.* Data sources: **W**=World Ozone and UV Data Centre  
 155 ([https://woude.org/archive/Archive-NewFormat/OzoneSonde\\_1.0\\_1/](https://woude.org/archive/Archive-NewFormat/OzoneSonde_1.0_1/)), **N**=Network for the  
 156 Detection of Atmospheric Composition Change (<ftp://ftp.cpc.ncep.noaa.gov/ndacc/station/>;  
 157 <ftp://ftp.cpc.ncep.noaa.gov/ndacc/RD/>), **E**= European Space Agency Validation Data Center  
 158 (<https://evdc.esa.int/> requires registration, or  
 159 <ftp://zardozi.nilu.no/nadir/projects/vintersol/data/o3sondes> requires account), **G**=Global  
 160 Monitoring Laboratory, National Oceanic and Atmospheric Administration  
 161 (<ftp://aftp.cmdl.noaa.gov/data/ozwv/Ozonesonde/>)

162 <sup>1</sup> Due to COVID-19 restrictions, most Canadian ozonesonde data were available only up to March or April 2020.

163 <sup>2</sup> Tateno data were corrected for the change from Carbon Iodine to ECC ozonesondes in December 2009.

164 <sup>3</sup> Stations affected by a drop-off in ECC sonde sensitivity > 3% in the stratosphere, after 2015 (see Stauffer et al.,  
 165 2020). The drop-off is much smaller (<< 1%) in the troposphere, and should be negligible here. At many of the  
 166 affected stations, ECC sondes behaved normally again in 2019/2020.

167

Station	Latitude (deg N)	Longitude (deg E)	Data source (see caption)	Data until	Profiles / spectra per month in 2020
Alert, Canada <sup>1,3</sup>	82.50	-62.34	W	4/2020	3.75
Eureka, Canada <sup>3</sup>	80.05	-86.42	W, E	9/2020	4.89
Ny-Ålesund, Norway	78.92	11.92	W, E	10/2020	7.10
<i>Ny-Ålesund FTIR, Norway</i>	78.92	11.92	<i>N</i>	7/2020	12.86
<i>Thule FTIR, Greenland</i>	76.53	-68.74	<i>N</i>	9/2020	73
Resolute, Canada <sup>1</sup>	74.72	-94.98	W	4/2020	5.50
Scoresbysund, Greenland	70.48	-21.95	E	11/2020	4.00
<i>Kiruna FTIR, Sweden</i>	67.41	20.41	<i>N</i>	7/2020	46
Sodankylä, Finland	67.36	26.63	W, E	12/2020	2.83
Lerwick, United Kingdom	60.13	-1.18	W, E	12/2020	3.92
Churchill, Canada <sup>1,3</sup>	58.74	-93.82	W	3/2020	3.33
Edmonton, Canada <sup>1,3</sup>	53.55	-114.10	W	3/2020	3.67
Goose Bay, Canada <sup>1</sup>	53.29	-60.39	W	3/2020	2.67
<i>Bremen FTIR, Germany</i>	53.13	8.85	<i>N</i>	10/2020	5.27
Legionowo, Poland	52.40	20.97	W	10/2020	4.00
Lindenberg, Germany	52.22	14.12	W	11/2020	4.73
DeBilt, Netherlands	52.10	5.18	W, E	12/2020	4.33
Valentia, Ireland	51.94	-10.25	W, E	12/2020	2.50

Uccle, Belgium	50.80	4.36	W, E	12/2020	12.00
Hohenpeissenberg, Germany	47.80	11.01	W	12/2020	10.50
<i>Zugspitze FTIR, Germany</i>	<i>47.42</i>	<i>10.98</i>	<i>N</i>	<i>9/2020</i>	<i>73</i>
<i>Jungfraujoch FTIR, Switzerland</i>	<i>46.55</i>	<i>7.98</i>	<i>N</i>	<i>12/2020</i>	<i>46</i>
Payerne, Switzerland	46.81	6.94	W	10/2020	11.10
Haute Provence, France	43.92	5.71	N	8/2020	2.50
<i>Haute Provence LIDAR, France</i>	<i>43.92</i>	<i>5.71</i>	<i>N</i>	<i>8/2020</i>	<i>3.50</i>
<i>Toronto FTIR, Canada</i>	<i>43.66</i>	<i>-79.40</i>	<i>N</i>	<i>10/2020</i>	<i>59</i>
Trinidad Head, California, USA	41.05	-124.15	G	12/2020	3.58
Madrid, Spain	40.45	-3.72	W	11/2020	4.09
Boulder, Colorado, USA	39.99	-105.26	G	12/2020	4.83
<i>Boulder FTIR, Colorado, USA</i>	<i>39.99</i>	<i>-105.26</i>	<i>N</i>	<i>10/2020</i>	<i>56</i>
Tateno (Tsukuba), Japan <sup>2</sup>	36.05	140.13	W	10/2020	2.70
<i>Table Mountain LIDAR, California, USA</i>	<i>34.40</i>	<i>-117.70</i>	<i>N</i>	<i>8/2020</i>	<i>19</i>
Izana, Tenerife, Spain	28.41	-16.53	W	8/2020	2.00
<i>Izana FTIR, Tenerife, Spain</i>	<i>28.30</i>	<i>-16.48</i>	<i>N</i>	<i>9/2020</i>	<i>28</i>
Hong Kong, China	22.31	114.17	W	9/2020	4.11
Hilo, Hawaii, USA <sup>3</sup>	19.72	-155.07	G	12/2020	4.08
<i>Mauna Loa FTIR, Hawaii, USA</i>	<i>19.54</i>	<i>-155.58</i>	<i>N</i>	<i>10/2020</i>	<i>36</i>
Paramaribo, Suriname	5.81	-55.21	N, E	10/2020	3.60
Pago Pago, American Samoa <sup>3</sup>	-14.25	-170.56	G	12/2020	3.08
Suva, Fiji <sup>3</sup>	-18.13	178.32	G	9/2020	1.44
<i>Wollongong FTIR, Australia</i>	<i>-34.41</i>	<i>150.88</i>	<i>N</i>	<i>10/2020</i>	<i>43</i>
Broadmeadows, Australia	-37.69	144.95	W	7/2020	4.29
Lauder, New Zealand	-45.04	169.68	W	10/2020	4.40
<i>Lauder FTIR, New Zealand</i>	<i>-45.04</i>	<i>169.68</i>	<i>N</i>	<i>10/2020</i>	<i>99</i>
Macquarie Island, Australia	-54.50	158.94	W	7/2020	4.29

168

169 Apart from the sondes, FTIR spectrometers from the Network for the Detection of  
170 Atmospheric Composition Change (NDACC, De Mazière et al., 2018) provide independent  
171 information, based on a completely different method (ground-based solar-infrared absorption  
172 spectrometry). The altitude resolution of FTIR ozone profiles in the troposphere is much coarser  
173 (5 to 10 km) than that of the sondes, while accuracy is similar, 5 to 10% (Vigouroux et al., 2015).  
174 Finally, we use data from tropospheric lidars (Gaudel et al., 2015, Granados-Muñoz & Leblanc  
175 2016), which provide ozone profiles from  $\approx 3$  to 12 km altitude, with accuracy comparable to the  
176 sondes (5 to 10%; Leblanc et al., 2018), and slightly coarser altitude resolution (100 m to 2 km).

177 We also use global atmospheric composition re-analyses from the Copernicus  
178 Atmosphere Monitoring Service for the years 2003 to 2019, and operational analyses for the year

179 2020 (CAMS, Inness et al., 2019; see also Park et al., 2020). The CAMS data are taken at the  
180 grid-points closest to the stations in Table 1. The analyses (in 2020) are adjusted for the small  
181 average difference to the re-analyses in 2018 and 2019. CAMS (re-)analyses are based on  
182 meteorological fields, and assimilation of satellite observations of ozone and NO<sub>2</sub>. However, for  
183 NO<sub>2</sub> the impact of the assimilation is small and frequently insignificant, so that tropospheric NO<sub>x</sub>  
184 in CAMS is essentially controlled by the prescribed emissions (Inness et al., 2019). Similarly, the  
185 limited information content of current satellite measurements of tropospheric ozone means that  
186 tropospheric ozone in CAMS is also driven largely by the prescribed emissions (and the  
187 chemistry module). Stratospheric ozone, however, is constrained well by the assimilated satellite  
188 data. Thus, CAMS analyses account for the large Arctic stratospheric depletion in spring of 2020  
189 (Manney et al., 2020; Wohltmann et al., 2020), for 2020 meteorological conditions, and for  
190 ozone transport, e.g. from the stratosphere to the troposphere (Neu et al., 2014). However, since  
191 they rely on “business as usual” emissions for 2020, the CAMS analyses do not account for the  
192 effects of COVID-19 emissions reductions in 2020 on tropospheric ozone (and NO<sub>x</sub>).

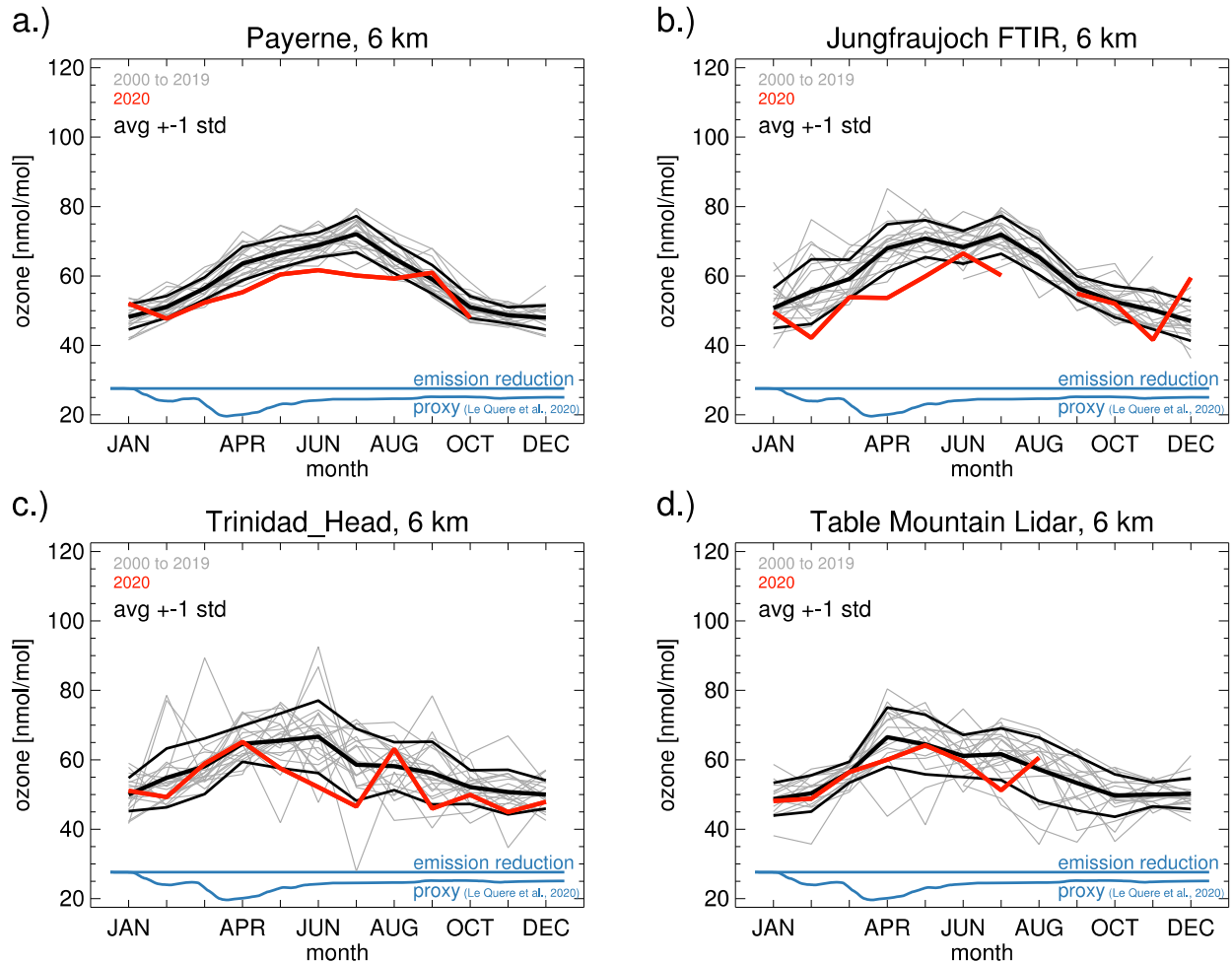
### 193 **3 Results**

194 For selected stations, Fig. 1 presents the annual cycles of tropospheric ozone over the last  
195 20 years, at 6 km, a representative altitude for the free troposphere. Monthly means (over 1-km  
196 wide layers) reduce synoptic meteorological variability and measurement noise, and focus on  
197 longer-term, larger-scale variations.

198 Payerne, Jungfraujoch, and Trinidad Head show an annual cycle with low ozone in  
199 winter and high ozone in summer. This is the case for most stations in the northern extratropics  
200 (Cooper et al., 2014; Gaudel et al., 2018; Parrish et al., 2020). Increased photochemical  
201 production due to more sunlight and warmer temperatures is the main driver for the summer  
202 ozone maximum in the northern extratropics (Wu et al., 2007; Archibald et al., 2020).

203 Figure 1 shows substantial yearly variability, but ozone levels are notably below average  
204 in 2020, at all four stations (thick red lines in Fig. 1). At Payerne and Jungfraujoch, and a number  
205 of other stations, monthly means in spring and summer 2020 were actually the lowest, or close to  
206 the lowest, since 2000. For context, the dark blue lines in Fig. 1 provide global CO<sub>2</sub> emission  
207 reductions due to the COVID-19 pandemic (Le Quéré et al., 2020b). Comparable reductions  
208 apply to global ozone precursor emissions (NO<sub>x</sub> and VOCs). The (daily) emission proxy in Fig. 1  
209 indicates that the largest effect for ozone might be expected after March 2020. However, Fig. 1  
210 does not show any clear or close correspondence between unusual ozone monthly means in 2020  
211 (red lines) and the emission reduction proxy (dark blue lines).

212



213

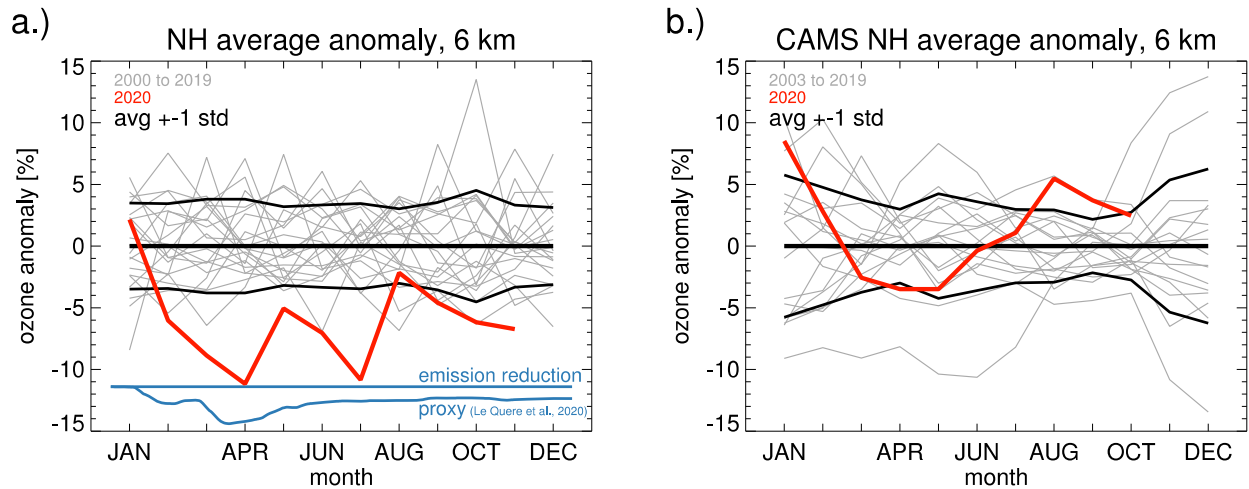
214 **Figure 1.** Observed ozone monthly means at four typical stations. Results are for 6 km altitude.  
 215 The thick red line highlights the year 2020. Climatological averages, and standard deviations  
 216 over the years 2000 to 2020 are indicated by the thick black lines. Payerne (a) and Trinidad Head  
 217 (c) are sonde stations. Jungfraujoch (b) is an FTIR station. Table Mountain (d) is a lidar station.  
 218 Dark blue lines: CO<sub>2</sub> emission reductions (arbitrary units) from Le Quéré et al. (2020b), as a  
 219 proxy for ozone precursor reductions in 2020.

220

221 Annual cycles of ozone anomalies, averaged over all northern extratropical stations  
 222 (stations north of 15°N), are shown in Fig. 2. Anomalies were defined as the relative deviation  
 223 (in percent) from the 2000-2020 climatological mean of each calendar month at each station. As  
 224 for the single stations in Fig. 1, the observed northern extratropical average shows exceptionally  
 225 low ozone throughout spring and summer 2020 (red line in Fig. 2a). This is not reproduced by  
 226 the CAMS analyses, which do not account for COVID-19 related emissions reductions, and  
 227 simulate ozone in the usual range in 2020 (red line in Fig. 2b). Again, there is no close temporal  
 228 correspondence between the unusual behavior of observed ozone in 2020 (red line in Fig. 2a),  
 229 and the emissions proxy (dark blue line in Fig. 2a).

230





231

232 **Figure 2.** Annual cycles of monthly mean northern extratropical ozone anomalies at 6 km  
 233 altitude. Anomalies are in percent, relative to the climatological monthly mean calculated for  
 234 each station/ instrument, and for the period 2000 to 2020 (all Januaries, all Februaries, ..., all  
 235 Decembers). These single station/instrument anomalies are then averaged over all northern  
 236 extratropical stations/instruments (north of 15°N). Panel **a)** Results from the station observations.  
 237 Panel **b)** Results for CAMS atmospheric composition (re-)analyses at grid points nearest the  
 238 stations. The CAMS data do not account for COVID-19 related emissions reductions in 2020.  
 239 Grey lines: individual years from 2000 to 2019. Thick red line: year 2020. Thick black lines:  
 240 average anomaly,  $\pm 1$  standard deviation over the years. Dark blue lines in panel a): Global CO<sub>2</sub>  
 241 emission reductions in 2020 (arbitrary units) from Le Quéré et al. (2020b), as in Fig. 1.

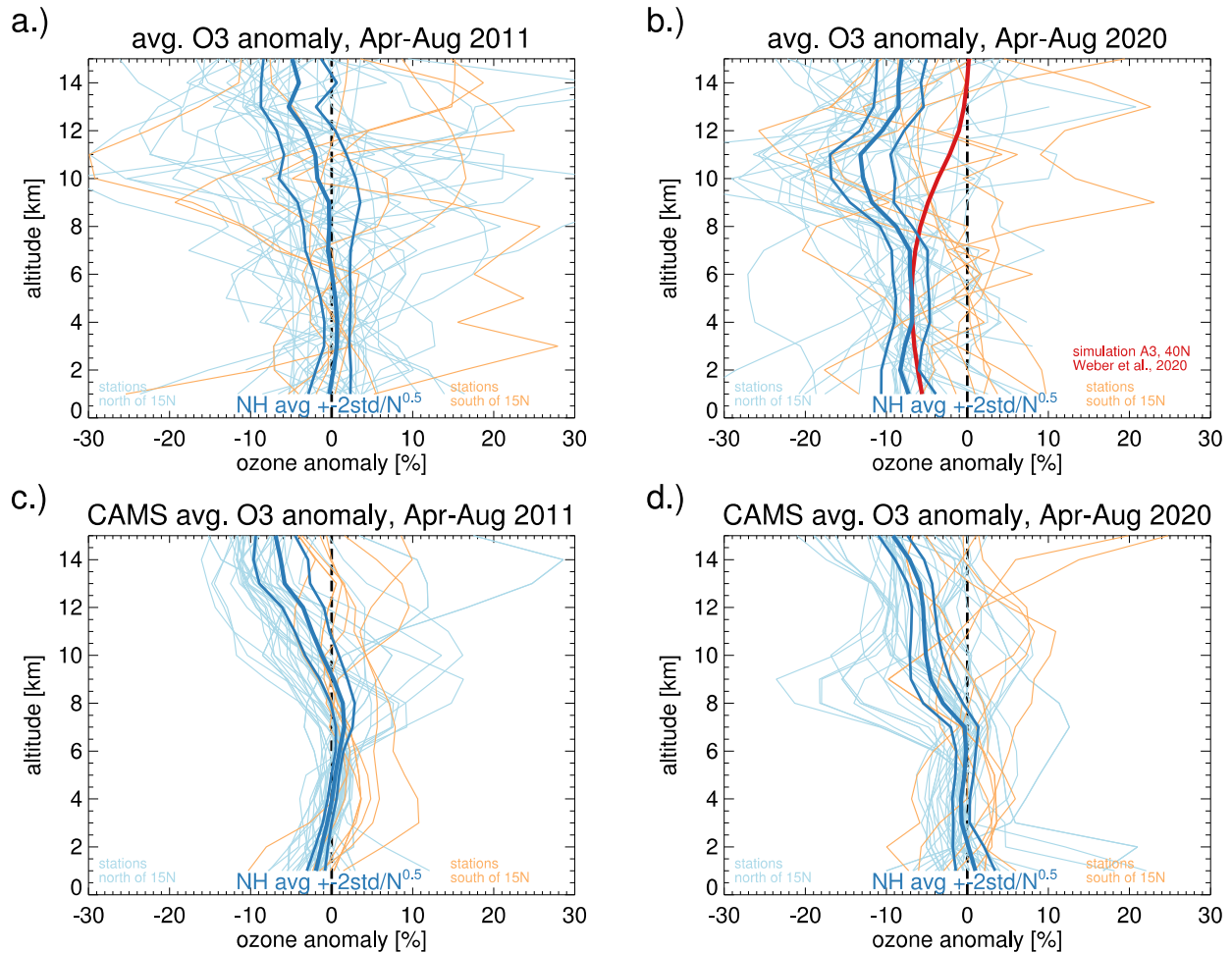
242

243 Figs. 1 and 2 show large negative anomalies from April to August 2020. Fig. 3 compares  
 244 anomaly profiles averaged over those five calendar months, between the years 2011 and 2020.  
 245 Both years saw unusually large springtime ozone depletion in the Arctic stratosphere (Manney et  
 246 al., 2020; Wohltmann et al., 2020). In the stratosphere, above  $\approx 10$  km, the Arctic depletion  
 247 appears as low ozone, both in observations and CAMS results (particularly for stations north of  
 248 50°N). In both the stratosphere and the troposphere, the observed profiles show more variability  
 249 than the smoother CAMS profiles. In 2020, most observed single station anomaly profiles (Fig.  
 250 3b) are negative throughout the northern extratropical troposphere (between 1 and 10 km). This  
 251 is not the case in 2011 (Fig. 3a, 3c), nor in the CAMS data in 2020 (Fig. 3d).

252 The 2020 anomaly is even clearer for the northern extratropical mean profile (dark blue  
 253 lines in Fig. 3). The observed 2020 mean anomaly profile is large, -6% to -9%, and statistically  
 254 significant at the 95% level (more than 99% in fact) from 1 to 8 km (Fig. 3b), whereas the  
 255 corresponding CAMS profile is close to zero (Fig. 3d). Fig. 3 indicates that Arctic stratospheric  
 256 springtime ozone depletion did not have a large effect on tropospheric ozone below 8 km in 2011  
 257 and 2020 (see also Fig. S1 in the supplement), and that the CAMS “business as usual” simulation  
 258 does not account for the observed large negative tropospheric anomaly in 2020.

259 Fig. 3b also shows a simulated profile of tropospheric ozone reduction from a recent  
 260 chemistry-climate modelling study of COVID-like emissions decreases by Weber et al. (2020).

261 This simulated profile (red line in our Fig 3b) matches the observed northern extratropical ozone  
 262 reduction (dark blue line), from the ground up to about 8 km. Above 8 km, the simulated profile  
 263 deviates by  $\approx 10\%$  from the observed profile, because it assumes fixed 2012 to 2014  
 264 meteorological conditions. The CAMS analyses (Fig. 3d) show that 2020 meteorological  
 265 conditions and springtime Arctic stratospheric ozone depletion resulted in ozone reductions of  
 266 5% to 10% above 9 km, consistent with the observations.



267

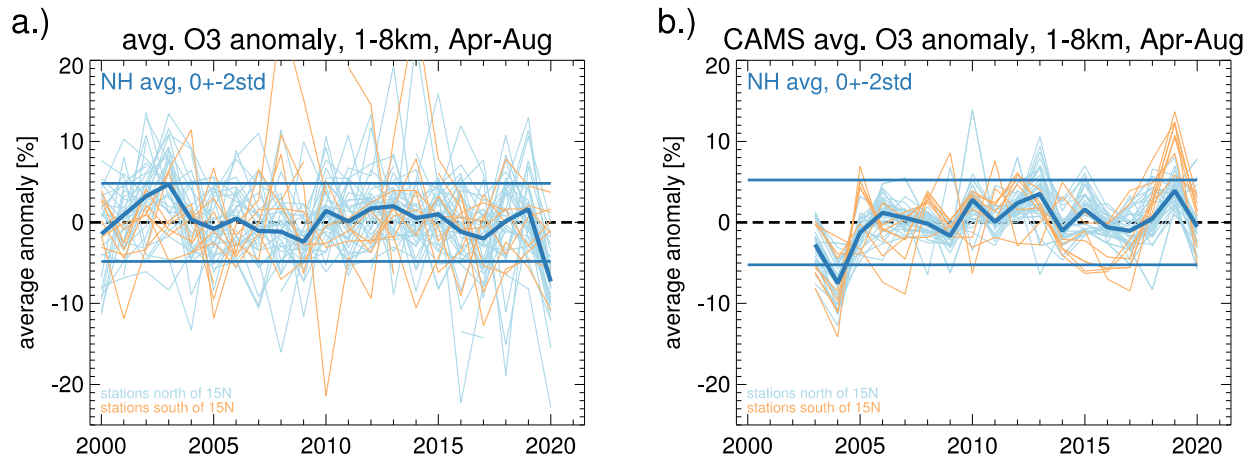
268 **Figure 3.** Ozone anomaly profiles (in percent), averaged over April to August. Stations are  
 269 excluded in years where their data cover less than three of these five months. Panel **a)** for the  
 270 year 2011. Panel **b)** for the year 2020. Light blue lines: northern extratropical stations (north of  
 271  $15^{\circ}\text{N}$ ). Light orange lines: remaining stations, south of  $15^{\circ}\text{N}$ . Thick dark blue line: mean of the  
 272 northern extratropical stations. Thin dark blue lines: 95% confidence interval of the mean of the  
 273 northern extratropical stations. Red line in panel **b)**: simulated ozone change at  $40^{\circ}\text{N}$  from Weber  
 274 et al. (2020; Fig. S4, scenario A3). Panels **c)**, **d)**: Same as a), b), but for CAMS (re-)analyses at  
 275 the grid-points closest to the stations.

276

277 Time series of the tropospheric anomaly (averaged from April to August, and from 1 to 8  
 278 km altitude) are shown in Fig. 4. In the observations (left panel), the year 2020 stands out with

279 large negative anomalies, not seen in the CAMS data. Across the twenty previous years, ozone  
 280 anomalies at individual stations (thin lines) are scattered around zero. The northern extratropical  
 281 average anomaly (dark blue line) is usually smaller than  $\pm 3\%$ . The only other observed exception  
 282 is the positive anomaly related to the (European) heat-wave summer of 2003 (Vautard et al.,  
 283 2007). The large negative northern extratropical anomaly in the observations in 2020,  $\approx -7\%$ , is  
 284 clearly outside of the  $\pm 2\sigma$  range of the previous 20 years (thin dark blue lines). It is not  
 285 reproduced by the CAMS “emissions as usual” analysis.

286

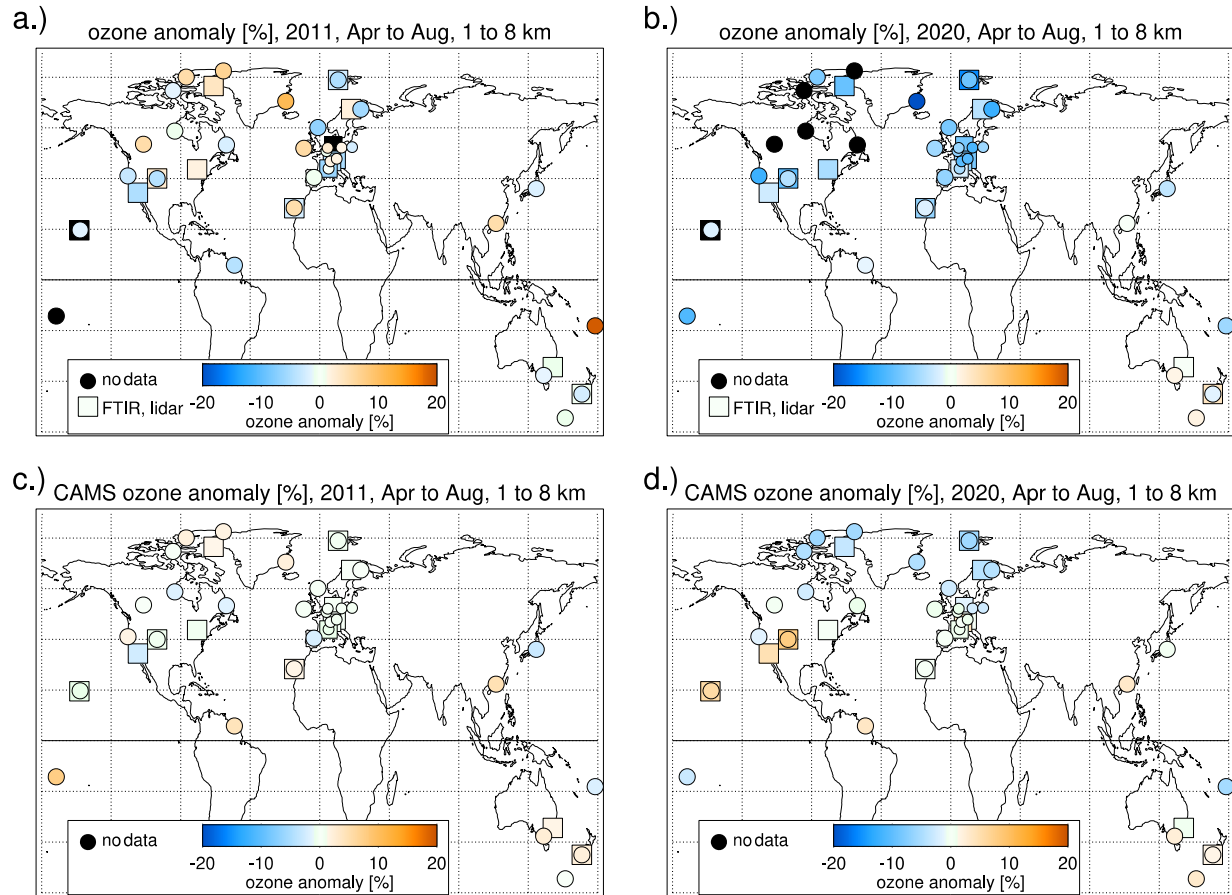


287

288 **Figure 4.** Tropospheric ozone anomaly, averaged over April to August and from 1 to 8 km, for  
 289 the years 2000 to 2020. Panel **a)** Observations. Panel **b)** CAMS atmospheric composition (re-  
 290 )analyses. Light blue lines: northern extratropical stations (north of  $15^\circ\text{N}$ ). Light orange lines:  
 291 stations south of  $15^\circ\text{N}$ . Thick dark blue line: Average over all stations north of  $15^\circ\text{N}$ . Thin dark  
 292 blue lines:  $\pm 2$  standard deviations over all years of this average.

293

294 The geographic distribution of the average tropospheric ozone anomalies is shown for  
 295 2011 and 2020 in Fig. 5. 2020 stands out in the observations with large negative anomalies at  
 296 nearly all northern extratropical stations, and a fairly uniform geographical distribution (see  
 297 Table S1 of the supplement for the numerical values). CAMS does show negative anomalies in  
 298 2020, but only north of  $50^\circ\text{N}$ , and not as large as the observations. In the Southern Hemisphere  
 299 in 2020, agreement between observations and CAMS is quite good, typically within 2.5% or  
 300 better (see also Table S1 in supplement). In 2011, some stations show positive anomalies,  
 301 negative anomalies are not as large as in 2020, and the geographical distribution is less uniform.  
 302 Agreement between observations and CAMS is reasonable in 2011, usually within a few percent.



303

304 **Figure 5.** Geographic distribution of observed tropospheric ozone anomalies (averaged over the  
 305 months April to August, and over altitudes from 1 to 8 km) for the years a) 2011 and b) 2020.  
 306 Panels c) and d): same, but for CAMS results at the station locations. Colored circles give the  
 307 anomaly at the ozonesonde stations. Squares are for FTIR and lidar stations. See Table S1 of the  
 308 supplement for the numerical values. Black filling indicates insufficient data in the given year.

309

#### 310 4 Discussion and Conclusions

311 Ozone stations in the northern extratropics indicate exceptionally low ozone in the free  
 312 troposphere (1 to 8 km) in spring and summer 2020. Compared to the 2000-2020 climatology,  
 313 ozone was reduced by 7% ( $\approx 4$  nmol/mol). Such widespread low tropospheric ozone, across so  
 314 many stations and over several months has not been observed in any previous year since 2000.  
 315 The observed 7% ozone reduction in the free troposphere stands in contrast to increases of  
 316 surface ozone by 10% to 30%, reported for many polluted urban areas after the COVID-19  
 317 related emissions reductions in 2020 (e.g., Collivignarelli et al., 2020; Lee et al., 2020; Shi &  
 318 Brasseur, 2020; Siciliano et al., 2020; Venter et al., 2020). However, the chemical regime for  
 319 ozone in the free troposphere is different (e.g., Kroll et al., 2020; Sillman, 1999; Thornton et al.,  
 320 2002), and free tropospheric ozone reductions are expected after the substantial decrease of  
 321 precursor emissions due to the COVID-19 pandemic (e.g. Guevara et al., 2020; Zhang et al.,  
 322 2020).

323 Recent model simulations of COVID-like emissions decreases (Weber et al., 2020) find  
324 tropospheric ozone reductions very similar to our observational results. From our results, and the  
325 simulations by Weber et al., 2020, it appears that the total tropospheric ozone burden of the  
326 northern extratropics decreased by about 7% for April to August 2020. The contribution from  
327 ozone increases in polluted urban areas to the total burden is opposite, but very small.

328 The Weber et al. (2020) simulations indicate that the major causes of tropospheric ozone  
329 reduction come from reduced surface transportation (ozone decrease throughout most of the  
330 northern extratropical troposphere), and from reduced aviation (ozone decrease mostly between  
331 10 and 12 km altitude and north of 30°N, see also Grewe et al., 2017). While the simulations are  
332 qualitatively consistent with the observations, they consider only March to May. New  
333 simulations using more recent and extended emissions estimates (Le Quéré et al., 2020b; Liu at  
334 al., 2020), and further comparison with our station observations would be worthwhile.

335 The observed large and fairly uniform 7% reduction of ozone in the northern  
336 extratropical troposphere in spring and summer 2020 provides a far reaching test case for the  
337 response of tropospheric ozone to emission changes. Further quantification of this anomaly will  
338 be possible, when observations from commercial aircraft (IAGOS), and satellite instruments  
339 become available. Additional modelling studies will improve our understanding of the  
340 contributions from different sectors such as air traffic, and surface transportation.

341

342

### 343 **Acknowledgments**

344 The authors greatly acknowledge the know-how and the hard work of station personnel  
345 launching the ozonesondes and taking the ground-based measurements. Without their dedicated  
346 efforts over many years, and especially during the COVID-19 lockdowns in 2020, investigations  
347 like this one are not possible!

### 348 **Funding acknowledgments**

349 Deutscher Wetterdienst funds the ozone program at Hohenpeißenberg and makes research like  
350 this possible.

351 NOAA GML supported additional launches in Boulder and Trinidad Head in April and May  
352 2020. NOAA and NASA's Upper Atmosphere Composition Observations (UACO) Program  
353 support the SHADOZ ozone soundings at Hilo, Pago-Pago (American Samoa) and Suva (Fiji).  
354 UACO also provides partial support for the Boulder FTIR and the Table Mountain Lidar.

355 The NDACC FTIR stations Bremen, Ny-Ålesund, Izaña, Kiruna, and Zugspitze have been  
356 supported by the German Bundesministerium für Wirtschaft und Energie (BMWi) via DLR  
357 under grants 50EE1711A, 50EE1711B, and 50EE1711D. Izaña, Kiruna, and Zugspitze have also  
358 been supported by the Helmholtz Society via the research program ATMO.

359 The FTIR measurements in Bremen and Ny-Ålesund receive additional support by the Senate of  
360 Bremen, the FTIR measurements in Ny-Ålesund also by AWI Bremerhaven. The University of  
361 Bremen further acknowledges funding by DFG (German research foundation) TRR 172 – Project  
362 Number 268020496 – within the Transregional Collaborative Research Center “Arctic



363 Amplification: Climate Relevant Atmospheric and Surface Processes, and Feedback  
364 Mechanisms (AC)3”.

365 The University of Liège contribution has been supported primarily by the Fonds de la Recherche  
366 Scientifique - FNRS under grant J.0147.18, as well as by the CAMS project. EM is a senior  
367 research associate of the F.R.S.-FNRS.

368 The Toronto FTIR measurements were supported by Environment and Climate Change Canada,  
369 the Natural Sciences and Engineering Research Council of Canada (NSERC), and the NSERC  
370 CREATE Training Program in Technologies for Exo-Planetary Science.

371 The University of the Wollongong thanks the Australian Research Council that has provided  
372 significant support over the years for the NDACC site at Wollongong, most recently as part of  
373 project DP160101598.

374 Part of this research work was carried out at the Jet Propulsion Laboratory, California Institute of  
375 Technology, under a contract with the National Aeronautics and Space Administration  
376 (80NM0018D004).

377 The National Center for Atmospheric Research is sponsored by the National Science Foundation.  
378 The NCAR FTS observation programs at Thule, GR and Boulder, CO are supported under  
379 contract by the National Aeronautics and Space Administration (NASA). The Thule work is also  
380 supported by the NSF Office of Polar Programs (OPP). We wish to thank the Danish  
381 Meteorological Institute for support at the Thule site and NOAA for support of the MLO site.

382 Key results for this manuscript were generated using Copernicus Atmosphere Monitoring  
383 Service Information from the European Community.

384 No author reports a financial (or other) conflict of interest.

### 385 **Data Sources**

386 Most of the ozonesonde data used in this study are freely available from the World Ozone and  
387 UV Data Centre (<https://woudc.org>) at Environment Canada (<https://exp-studies.tor.ec.gc.ca/>),  
388 and are downloadable at [https://woudc.org/archive/Archive-NewFormat/OzoneSonde\\_1.0\\_1/](https://woudc.org/archive/Archive-NewFormat/OzoneSonde_1.0_1/)).

389 Some ozonesonde data for 2020 were not yet available at the WOUDC. Instead, rapid delivery  
390 data were obtained from <ftp://zardoz.nilu.no/nadir/projects/vintersol/data/o3sondes> (requires  
391 registration), at the Nadir database of the Norwegian Institute for Air Quality (NILU,  
392 <https://projects.nilu.no/nadir/obs.html>). Registration information, and the same data in a  
393 different format, are available from the European Space Agency Validation Data Center  
394 (<https://evdc.esa.int/>).

395 For Boulder, Trinidad Head, Hilo, Fiji, and Samoa, stations operated by the US National Oceanic  
396 and Atmospheric Administration, Global Monitoring Laboratory  
397 (<https://www.esrl.noaa.gov/gmd/ozwv/>), data can be obtained freely from  
398 <ftp://aftp.cmdl.noaa.gov/data/ozwv/Ozonesonde/>.

399 FTIR and lidar data, as well as some ozonesonde data, are from the Network for the Detection of  
400 Atmospheric Composition Change (<https://ndacc.org>), and are freely available at  
401 <ftp://ftp.cpc.ncep.noaa.gov/ndacc/station/> and <ftp://ftp.cpc.ncep.noaa.gov/ndacc/RD/>.

402 Copernicus Atmosphere Monitoring Service (CAMS) global chemical weather EAC4 re-  
403 analyses are available at <https://atmosphere.copernicus.eu/data> . CAMS operational global  
404 analyses and forecasts are available at <https://apps.ecmwf.int/datasets/data/cams-nrealtime/> .

## 405 References

- 406 Archibald, A.T., Neu, J.L., Elshorbany, Y., Cooper, O.R., Young, P.J., Akiyoshi, H., et al. (2020).  
407 Tropospheric Ozone Assessment Report: A critical review of changes in the tropospheric ozone  
408 burden and budget from 1850-2100. *Elementa Science of the Anthropocene*, **8**, 034.  
409 <https://doi.org/10.1525/elementa.2020.034>
- 410 Barré, J., Petetin, H., Colette, A., Guevara, M., Peuch, V.-H., Rouil, L., et al. (in review, 2020).  
411 Estimating lockdown induced European NO<sub>2</sub> changes. *Atmospheric Chemistry and Physics*  
412 *Discussions*. <https://doi.org/10.5194/acp-2020-995>
- 413 Bauwens, M., Compernelle, S., Stavrakou, T., Müller, J.-F., van Gent, J., Eskes, H., et al. (2020).  
414 Impact of coronavirus outbreak on NO<sub>2</sub> pollution assessed using TROPOMI and OMI  
415 observations. *Geophysical Research Letters*, **47**, e2020GL087978.  
416 <https://doi.org/10.1029/2020GL087978>
- 417 Bozem, H., Butler, T. M., Lawrence, M. G., Harder, H., Martinez, M., Kubistin, D., et al. (2017).  
418 Chemical processes related to net ozone tendencies in the free troposphere. *Atmospheric*  
419 *Chemistry and Physics*, **17**, 10565–10582, <https://doi.org/10.5194/acp-17-10565-2017>
- 420 Chen, L.-W. A., Chien, L.-C., Li, Y., and Lin, G. (2020). Nonuniform impacts of COVID-19  
421 lockdown on air quality over the United States, *Science of The Total Environment*, **745**, 141105.  
422 <https://doi.org/10.1016/j.scitotenv.2020.141105>
- 423 Collivignarelli, M.C., Abbà, A., Bertanza, G., Pedrazzani, R., Ricciardi, P., & Carnevale Miino,  
424 M. (2020). Lockdown for CoViD-2019 in Milan: What are the effects on air quality? *Science of*  
425 *the Total Environment*, **732**, 139280. <https://doi.org/10.1016/j.scitotenv.2020.139280>
- 426 Cooper, O.R., Parrish, D.D., Ziemke, J., Balashov, N.V., Cupeiro, M., Galbally, I.E., et al.  
427 (2014). Global distribution and trends of tropospheric ozone: An observation-based review.  
428 *Elementa: Science of the Anthropocene*, **2**, 000029.  
429 <https://doi.org/10.12952/journal.elementa.000029>
- 430 De Mazière, M., Thompson, A. M., Kurylo, M. J., Wild, J. D., Bernhard, G., Blumenstock, T., et  
431 al. (2018). The Network for the Detection of Atmospheric Composition Change (NDACC):  
432 history, status and perspectives. *Atmospheric Chemistry and Physics*, **18**, 4935–4964.  
433 <https://doi.org/10.5194/acp-18-4935-2018>
- 434 Dentener F., T. Keating, T., & Akimoto, H. (eds.) (2011). *Hemispheric Transport of Air Pollution*  
435 *2010, Part A: Ozone and Particulate Matter*. Air Pollution Studies No. 17, United Nations, New  
436 York and Geneva, ISSN 1014-4625, ISBN 978-92-1-117043-6. [Available online at  
437 <http://www.unece.org/index.php?id=25381> ]
- 438 Ding, J., van der A, R. J., Eskes, H. J., Mijling, B., Stavrakou, T., van Geffen, J. H. et al. (2020).  
439 NO<sub>x</sub> emissions reduction and rebound in China due to the COVID-19 crisis. *Geophysical*  
440 *Research Letters*, **46**, e2020GL089912. <https://doi.org/10.1029/2020GL089912>

- 441 Feng, S., Jiang, F., Wang, H., Wang, H., Ju, W., Shen, Y., et al. (2020). NO<sub>x</sub> emission changes  
442 over China during the COVID-19 epidemic inferred from surface NO<sub>2</sub> observations. *Geophysical*  
443 *Research Letters*, **47**, e2020GL090080. <https://doi.org/10.1029/2020GL090080>
- 444 Gaudel, A., Ancellet, G., & Godin-Beekmann, S. (2015). Analysis of 20 years of tropospheric  
445 ozone vertical profiles by lidar and ECC at Observatoire de Haute Provence (OHP) at 44°N,  
446 6.7°E. *Atmospheric Environment*, **113**, 78-89. <https://doi.org/10.1016/j.atmosenv.2015.04.028>
- 447 Gaudel, A., Cooper, O.R., Ancellet, G., Barret, B., Boynard, A., Burrows, J.P., et al. (2018).  
448 Tropospheric Ozone Assessment Report: Present-day distribution and trends of tropospheric  
449 ozone relevant to climate and global atmospheric chemistry model evaluation. *Elementa Science*  
450 *of the Anthropocene*, **6**, 39. <https://doi.org/10.1525/elementa.291>
- 451 Gelaro, R., McCarty, W., Suarez, M. J., Todling, R., Molod, A., Takacs, et al. (2017). The  
452 Modern-Era Retrospective Analysis for Research and Applications, version 2 (MERRA-2).  
453 *Journal of Climate*, **30**, 5419–5454. <https://doi.org/10.1175/JCLI-D-16-0758.1>
- 454 Goldberg, D. L., Anenberg, S. C., Griffin, D., McLinden, C. A., Lu, Z., & Streets, D. G. (2020).  
455 Disentangling the impact of the COVID-19 lockdowns on urban NO<sub>2</sub> from natural variability.  
456 *Geophysical Research Letters*, **47**, e2020GL089269. <https://doi.org/10.1029/2020GL089269>
- 457 Granados-Muñoz, M. J., & Leblanc, T. (2016). Tropospheric ozone seasonal and long-term  
458 variability as seen by lidar and surface measurements at the JPL-Table Mountain Facility,  
459 California. *Atmospheric Chemistry and Physics*, **16**, 9299–9319. [https://doi.org/10.5194/acp-16-](https://doi.org/10.5194/acp-16-9299-2016)  
460 [9299-2016](https://doi.org/10.5194/acp-16-9299-2016)
- 461 Grewe, V., Dahlmann, K., Flink, J., Frömming, C., Ghosh, R., Gierens, et al. (2017). Mitigating  
462 the Climate Impact from Aviation: Achievements and Results of the DLR WeCare Project.  
463 *Aerospace*, **4**, 34, <https://doi.org/10.3390/aerospace4030034>
- 464 Guevara, M., Jorba, O., Soret, A., Petetin, H., Bowdalo, D., Serradell, K., et al. (2020, accepted).  
465 Time-resolved emission reductions for atmospheric chemistry modelling in Europe during the  
466 COVID-19 lockdowns. *Atmospheric Chemistry and Physics*. [https://doi.org/10.5194/acp-2020-](https://doi.org/10.5194/acp-2020-686)  
467 [686](https://doi.org/10.5194/acp-2020-686)
- 468 Hurtmans, D., Coheur, P.-F., Wespes, C., Clarisse, L., Scharf, O., Clerbaux, C., et al. (2012).  
469 FORLI radiative transfer and retrieval code for IASI. *Journal of Quantitative Spectroscopy and*  
470 *Radiative Transfer*, **113** (11), 1391-1408. <https://doi.org/10.1016/j.jqsrt.2012.02.036>.
- 471 Inness, A., Ades, M., Agustí-Panareda, A., Barré, J., Benedictow, A., Blechschmidt, A.M., et al.  
472 (2019). The CAMS reanalysis of atmospheric composition. *Atmospheric Chemistry and Physics*,  
473 **19**, 3515–3556. <https://doi.org/10.5194/acp-19-3515-2019>
- 474 Keller, C. A., Evans, M. J., Knowland, K. E., Hasenkopf, C. A., Modekurty, S., Lucchesi, et al.  
475 (in review, 2020). Global Impact of COVID-19 Restrictions on the Surface Concentrations of  
476 Nitrogen Dioxide and Ozone. *Atmospheric Chemistry and Physics Discussions*.  
477 <https://doi.org/10.5194/acp-2020-685>
- 478 Kroll, J.H., Heald, C.L., Cappa, C.D., Farmer, D.K., Fry, J.L., Murphy, J.G., & Steiner, A.L.  
479 (2020). The complex chemical effects of COVID-19 shutdowns on air quality. *Nature Chemistry*,  
480 **12**, 777–779. <https://doi.org/10.1038/s41557-020-0535-z>



- 481 Leblanc, T., Brewer, M. A., Wang, P. S., Granados-Muñoz, M. J., Strawbridge, K. B., Travis, M.,  
482 et al. (2018). Validation of the TOLNet lidars: the Southern California Ozone Observation  
483 Project (SCOOP). *Atmospheric Measurement Techniques*, **11**, 6137–6162.  
484 <https://doi.org/10.5194/amt-11-6137-2018>
- 485 Lee, J. D., Drysdale, W. S., Finch, D. P., Wilde, S. E., & Palmer, P. I. (2020). UK surface NO<sub>2</sub>  
486 levels dropped by 42 % during the COVID-19 lockdown: impact on surface O<sub>3</sub>. *Atmospheric  
487 Chemistry and Physics*, **20**, 15743–15759. <https://doi.org/10.5194/acp-20-15743-2020>
- 488 Le Quéré, C., Jackson, R.B., Jones, M.W., Smith, A.J.P., Abernethy, S., Andrew, R.M., et al.  
489 (2020a). Temporary reduction in daily global CO<sub>2</sub> emissions during the COVID-19 forced  
490 confinement. *Nature Climate Change*, **10**, 647–653. <https://doi.org/10.1038/s41558-020-0797-x>
- 491 Le Quéré, C., Jackson, R.B., Jones, M.W., Smith, A.J.P., Abernethy, S., Andrew, R.M., et al.  
492 (2020b). Supplementary data to: Le Quéré et al (2020), Temporary reduction in daily global CO<sub>2</sub>  
493 emissions during the COVID-19 forced confinement (Version 1.2). *Global Carbon Project*.  
494 <https://doi.org/10.18160/RQDW-BTJU>
- 495 Liu, X., Bhartia, P. K., Chance, K., Spurr, R.J.D., & Kurosu, T. P. (2010). Ozone profile  
496 retrievals from the Ozone Monitoring Instrument. *Atmospheric Chemistry and Physics*, **10**,  
497 2521–2537. <https://doi.org/10.5194/acp-10-2521-2010>
- 498 Liu, Z., Ciais, P., Deng, Z., Lei, R., Davis, S. J., Feng, S., et al. (2020). Near-real-time  
499 monitoring of global CO<sub>2</sub> emissions reveals the effects of the COVID-19 pandemic. *Nature  
500 Communications*, **11**, 5172. <https://doi.org/10.1038/s41467-020-18922-7>
- 501 Manney, G. L., Livesey, N. J., Santee, M. L., Froidevaux, L., Lambert, A., Lawrence, Z. D., et al.  
502 (2020). Record-low Arctic stratospheric ozone in 2020: MLS observations of chemical processes  
503 and comparisons with previous extreme winters. *Geophysical Research Letters*, **47**,  
504 e2020GL089063. <https://doi.org/10.1029/2020GL089063>
- 505 Menut, L., Bessagnet, B., Siour, G., Mailler, S., Pennel, R., & Cholakian, A. (2020). Impact of  
506 lockdown measures to combat Covid-19 on air quality over western Europe. *Science of The Total  
507 Environment*, **741**, 140426. <https://doi.org/10.1016/j.scitotenv.2020.140426>
- 508 Nédélec, P., Blot, R., Boulanger, D., Athier, G., Cousin, J-M., Gautron, B., et al. (2015).  
509 Instrumentation on commercial aircraft for monitoring the atmospheric composition on a global  
510 scale: the IAGOS system, technical overview of ozone and carbon monoxide measurements.  
511 *Tellus B: Chemical and Physical Meteorology*, **67**(1). <https://doi.org/10.3402/tellusb.v67.27791>
- 512 Neu, J., Flury, T., Manney, G., Santee, M.L., Livesey N.J., & Worden, J. (2014). Tropospheric  
513 ozone variations governed by changes in stratospheric circulation. *Nature Geoscience*, **7**, 340–  
514 344. <https://doi.org/10.1038/ngeo2138>
- 515 Oetjen, H., Payne, V. H., Kulawik, S. S., Eldering, A., Worden, J., Edwards, D. P., et al. (2014).  
516 Extending the satellite data record of tropospheric ozone profiles from Aura-TES to MetOp-  
517 IASI: characterisation of optimal estimation retrievals. *Atmospheric Measurement Techniques*, **7**,  
518 4223–4236. <https://doi.org/10.5194/amt-7-4223-2014>
- 519 Ordóñez, C., Garrido-Perez, J.M., & García-Herrera, R. (2020). Early spring near-surface ozone  
520 in Europe during the COVID-19 shutdown: Meteorological effects outweigh emission changes.  
521 *Science of the Total Environment*, **747**, 141322. <https://doi.org/10.1016/j.scitotenv.2020.141322>

- 522 Park, S., Son, S.-W., Jung, M.-I., Park, J., & Park, S.-S. (2020). Evaluation of tropospheric ozone  
523 reanalyses with independent ozonesonde observations in East Asia. *Geoscience Letters*, **7**, 12.  
524 <https://doi.org/10.1186/s40562-020-00161-9>
- 525 Parrish, D.D., Derwent, R.G., Steinbrecht, W., Stübi, R., Van Malderen, R., Steinbacher, M., et  
526 al. (2020). Zonal similarity of long-term changes and seasonal cycles of baseline ozone at  
527 northern midlatitudes. *Journal of Geophysical Research: Atmospheres*, **125**, e2019JD031908.  
528 <https://doi.org/10.1029/2019JD031908>
- 529 Sicard, P., De Marco, A., Agathokleous, E., Feng, Z., Xu, X., Paoletti, E., et al. (2020). Amplified  
530 ozone pollution in cities during the COVID-19 lockdown, *Science of the Total Environment*, **735**,  
531 139542. <https://doi.org/10.1016/j.scitotenv.2020.139542>
- 532 Siciliano, B., Dantas, G., da Silva, C. M., & Arbilla G. (2020). Increased ozone levels during the  
533 COVID-19 lockdown: Analysis for the city of Rio de Janeiro, Brazil, *Science of the Total*  
534 *Environment*, **737**, 139765. <https://doi.org/10.1016/j.scitotenv.2020.139765>
- 535 Sillman, S., (1999). The relation between ozone, NO<sub>x</sub> and hydrocarbons in urban and polluted  
536 rural environments. *Atmospheric Environment*, **33**(12), 1821-1845.  
537 [https://doi.org/10.1016/S1352-2310\(98\)00345-8](https://doi.org/10.1016/S1352-2310(98)00345-8)
- 538 Shi, X., & Brasseur, G. P. (2020). The response in air quality to the reduction of Chinese  
539 economic activities during the COVID-19 outbreak. *Geophysical Research Letters*, **47**,  
540 e2020GL088070. <https://doi.org/10.1029/2020GL088070>
- 541 Smit, H.G.J., Straeter, W., Johnson, B., Oltmans, S., Davies, J., Tarasick, D.W., et al. (2007).  
542 Assessment of the performance of ECC-ozonesondes under quasi-flight conditions in the  
543 environmental simulation chamber: Insights from the Jülich Ozone Sonde Intercomparison  
544 Experiment (JOSIE). *Journal of Geophysical Research*, **112**, D19306.  
545 <https://doi.org/10.1029/2006JD007308>
- 546 Stauffer, R.M., Thompson, A.M., Kollonige, D.E., Witte, J.C., Tarasick, D.W., Davies, J., et al.  
547 (2020). A post-2013 dropoff in total ozone at a third of global ozonesonde stations:  
548 Electrochemical concentration cell instrument artifacts? *Geophysical Research Letters*, **47**,  
549 e2019GL086791. <https://doi.org/10.1029/2019GL086791>
- 550 Sterling, C.W., Johnson, D.J., Oltmans, S.J., Smit, H.G.J., Jordan, A.F., Cullis, P.D., et al. (2018).  
551 Homogenizing and estimating the uncertainty in NOAA's long-term vertical ozone profile  
552 records measured with the electrochemical concentration cell ozonesonde. *Atmospheric*  
553 *Measurement Techniques*, **11**, 3661-3687. <https://doi.org/10.5194/amt-11-3661-2018>
- 554 Strahan, S. E., Douglass, A. R., & Damon, M. R. (2019). Why do Antarctic ozone recovery  
555 trends vary? *Journal of Geophysical Research: Atmospheres*, **124**, 8837–8850.  
556 <https://doi.org/10.1029/2019JD030996>
- 557 Tarasick, D.W., Davies, J., Smit, H.G.J., & Oltmans, S.J. (2016). A re-evaluated Canadian  
558 ozonesonde record: measurements of the vertical distribution of ozone over Canada from 1966 to  
559 2013. *Atmospheric Measurement Techniques*, **9**, 195-214. [https://doi.org/10.5194/amt-9-195-](https://doi.org/10.5194/amt-9-195-2016)  
560 [2016](https://doi.org/10.5194/amt-9-195-2016).
- 561 Tarasick, D., Galbally, I.E., Cooper, O.R., Schultz, M.G., Ancellet, G., Leblanc, T., et al. (2019).  
562 Tropospheric Ozone Assessment Report: Tropospheric ozone from 1877 to 2016, observed

- 563 levels, trends and uncertainties. *Elementa Science of the Anthropocene*, **7**(1).  
564 <https://doi.org/10.1525/elementa.376>
- 565 Thornton, J.A., Wooldridge, P.J., Cohen, R.C., Martinez, M., Harder, H., Brune, W. H., et al.  
566 (2002). Ozone production rates as a function of NO<sub>x</sub> abundances and HO<sub>x</sub> production rates in  
567 Nashville urban plume. *Journal of Geophysical Research*, **107** (D12).  
568 <https://doi.org/10.1029/2001JD000932>
- 569 Van Malderen, R., Allaart, M. A. F., De Backer, H., Smit, H. G. J., & De Muer, D. (2016). On  
570 instrumental errors and related correction strategies of ozonesondes: possible effect on calculated  
571 ozone trends for the nearby sites Uccle and De Bilt. *Atmospheric Measurement Techniques*, **9**,  
572 3793–3816. <https://doi.org/10.5194/amt-9-3793-2016>
- 573 Vautard, R., Beekmann, M., Desplat, J., Hodzic, A., & Morel, S. (2007). Air quality in Europe  
574 during the summer of 2003 as a prototype of air quality in a warmer climate. *Comptes Rendus*  
575 *Geoscience*, **339**, 747–763. <https://doi.org/10.1016/j.crte.2007.08.003>
- 576 Venter, Z. S., Aunan, K., Chowdhury, S., & Lelieveld, J. (2020). COVID-19 lockdowns cause  
577 global air pollution declines. *Proceedings of the National Academy of Sciences*, **117** (32), 18984–  
578 18990. <https://doi.org/10.1073/pnas.2006853117>
- 579 Vigouroux, C, Blumenstock, T, Coffey, M, Errera, Q, García, O, Jones, N.B, et al. (2015). Trends  
580 of ozone total columns and vertical distribution from FTIR observations at eight NDACC  
581 stations around the globe. *Atmospheric Chemistry and Physics*, **15**, 2915–2933.  
582 <https://doi.org/10.5194/acp-15-2915-2015>
- 583 Weber, J., Shin, Y. M., Staunton Sykes, J., Archer-Nicholls, S., Abraham, N. L., & Archibald, A.  
584 T. (2020). Minimal climate impacts from short-lived climate forcers following emission  
585 reductions related to the COVID-19 pandemic. *Geophysical Research Letters*, **47**,  
586 e2020GL090326. <https://doi.org/10.1029/2020GL090326>
- 587 Witte, J. C., Thompson, A.M., Smit, H.G.J., Fujiwara, M., Posny, F., Coetzee G.J.R., et al.  
588 (2017). First reprocessing of Southern Hemisphere ADDitional OZonesondes (SHADOZ) profile  
589 records (1998–2015): 1. Methodology and evaluation. *Journal of Geophysical Research:*  
590 *Atmospheres*, **122**, 6611– 6636. <https://doi.org/10.1002/2016JD026403>
- 591 WMO (2014), *Quality assurance and quality control for ozonesonde measurements in GAW*,  
592 World Meteorological Organization (WMO), Global Atmosphere Watch report series, Smit,  
593 H.G.J., and ASOPOS panel (eds.), GAW Report No. 201, 100 pp., Geneva. [Available online at  
594 [https://library.wmo.int/doc\\_num.php?explnum\\_id=7167](https://library.wmo.int/doc_num.php?explnum_id=7167) ]
- 595 Wohltmann, I., von der Gathen, P., Lehmann, R., Maturilli, M., Deckelmann, H., Manney, G. L.,  
596 et al. (2020). Near-complete local reduction of Arctic stratospheric ozone by severe chemical  
597 loss in spring 2020. *Geophysical Research Letters*, **47**, e2020GL089547.  
598 <https://doi.org/10.1029/2020GL089547>
- 599 Wu, S., Mickley, L. J., Jacob, D. J., Logan, J. A., Yantosca, R. M., & Rind, D. (2007). Why are  
600 there large differences between models in global budgets of tropospheric ozone? *Journal of*  
601 *Geophysical Research*, **112**, D05302. <https://doi.org/10.1029/2006JD007801>
- 602 Zhang, Y., West, J. J., Emmons, L. K., Flemming, J., Jonson, J. E., Lund, M. T., et al. (2020).  
603 Contributions of world regions to the global tropospheric ozone burden change from 1980 to

604 2010. *Geophysical Research Letters*, **47**, e2020GL089184.  
605 <https://doi.org/10.1029/2020GL089184>